The Design of Advanced Gamut Mapping Algorithms in Color Management Systems

Mei-Chun Lo[*], Hung-Shin Chen [*], Chia-Pin Chueh [*]

Key Words: Device Independent Color, Color Gamut, Color Appearance, Gamut Mapping Algorithms, Clipping, Linear Compression, Non-linear Compression, Focal Points, Color Management System.

Abstract: Currently the design for Color Management System (CMS) is based on the concept of Device Independent Color to implement the optimal color imaging across different imaging devices. However, the color appearance may not match between source and destination images although compared under the same viewing conditions. It is due to the dissimilar color gamuts existed between these two imaging devices used. Therefore it is needed to apply an optimal Gamut Mapping Algorithm (GMA) in a CMS process.

The objective of this study is to derive GMAs to overcome the color-imaging problem caused by the mismatch of color gamuts in cross-media environments. Two imaging devices of a Hi-Fi monitor and an Inkjet printer were tested.

The GMAs derived here, by taking into account of false boundary problem, directly carried out in a uniform 3D color space without any constraint, were categorized into two types of single-focal-point (SFP), and multiple-focal-points (MFP). Separately each type also carried out three approaches of clipping, linear compression and nonlinear compression. The SFP models used L*= 50 as the single focal point, whereas the MFP ones applied focal points repectively on three parts of highlight, mid-tone, and shadow. Before applying MFP method, a S-type scale method was implemented to change gamut distributions of originals tested. The S-type scale method let both the original and the reproduction gamuts have the same lightness range but optimally kept the original shadow areas of gradation.

An advanced evaluation of models performance, by adopting a forced-choice paired-comparison experiment, was carried out using both of complex and computer-graphic color images.

[*] Dept. of Graphic Communications and Technology, Shih Hsin University, Taiwan, R.O.C.

Results showed that the GMA, coupled with both of non-linear 3-D gamut compression and multiple-mapping-directions approaches, introduced better renditions than other five models tested. Especially it was more evident to complex images, but less evident to CG images having fewer gradations. Also the non-linear gamma-compression method minimized the loss of details occurred in clipping, while retained the merit of accurately reproducing most of common gamut colors.

INTRODUCTION

Various recent color management systems (CMSs) on the market have realized device-independent color environment, consistent color reproduction across different media.

However, some technical factors need to be considered in current CMSs in order to maintain the appearance of the original image when the image data are transferred and processed across different imaging media/devices. One of which is the gamut difference between dissimilar devices, which utilize different sets of primaries to produce images. Among the variety of devices, the gamut mismatch is most noticeable between a CRT monitor and a hardcopy printer. The focus of this research, hence, is to propose an optimal approach to overcome these gamut differences. It is what is commonly referred to as *color-gamut mapping*.

For a typical printer, the gamut range in CIELAB color space is usually only 50 to 80 percent of that of a typical CRT monitor. For this reason, it is impossible for the printer to reproduce all the colors of the monitor. Hence there is necessity to map out-of-gamut colors of the monitor to the inside of the printer gamut, while minimizing changes of color appearance in images. The purpose of gamut mapping is to preserve the color appearance of an image as mush as possible when the image is reproduced by a different device or medium.

Although the research of 2D gamut mapping algorithms (GMAs) built on Lightness-Chroma planes is active, ideally the GMA approach should work in a 3D uniform color space (CIELAB) directly. However, few studies, based on the combination of 3D GMA methods and image dependence, are known. Thus, the development of 3D GMAs based on the concept of image dependency is necessary (Katoh et al. 1999).

GAMUT MAPPING ALGOROTHMS (GMAs)

A variety of gamut-mapping techniques have been suggested, but a generalized, automated algorithm that can be used for various applications has yet to be developed. Now, the trend of GMA approach is required to work in a 3D uniform color space based on the concept of image-dependency directly.

A few issues were taken into account in this study when designing 3D GMA approaches. Those issues considered include: 1) 3D description of gamut shell; 2) 3D formation of color gamut; 3) types of mapping, including clipping, linear compression, and nonlinear compression; 4) mapping directions, including single-focal-point and multiple-focal-points; and 5) cross points on gamut surface.

(1) 3D formation of color gamut

Monitor gamut

A set of {a*, b*, L*} initial data was generated with equal intervals of $\Delta a^*=5$, $\Delta b^*=5$, and $\Delta L^*=5$ in the range of $-120 \le a^* \le 120$, $-120 \le b^* \le 120$, and $0 \le L^* \le 100$ respectively in the CIE L*a*b* uniform color space.

The corresponding initial RGB data had been limited within the sRGB range and located between 0 and 1. Thus the corresponding {a*b*L*} values filling the sRGB space were used to define sRGB monitor's gamut (Figure 1).

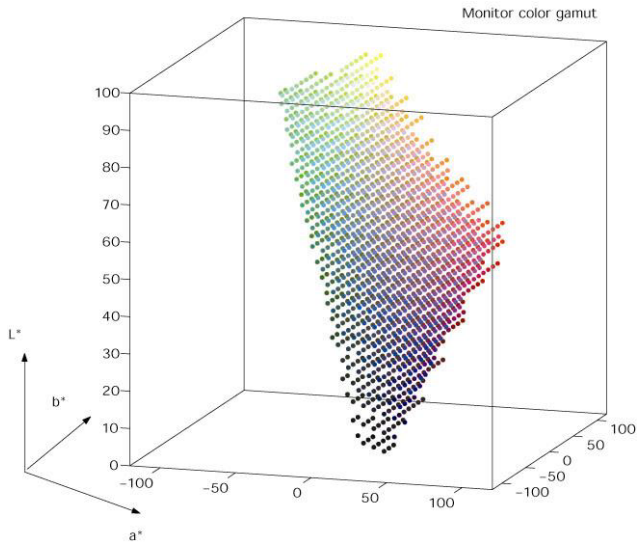

Figure 1 Color gamut of the sRGB monitor tested

Printer gamut

A set of {R, G, B} initial data was generated using a computer in terms of 15 DAC interval for each channel of R, G, and B, ranging from 0 to 255 values. The RGB cube data set, rendered as 18×18×18 matrix of color chips, was then produced using a 4-color inkjet printer, and measured using a Gretag

spectrophotometer to obtain XYZ tristimulus values against the D_{65} light source used in viewing hardcopies tested in the experiments.

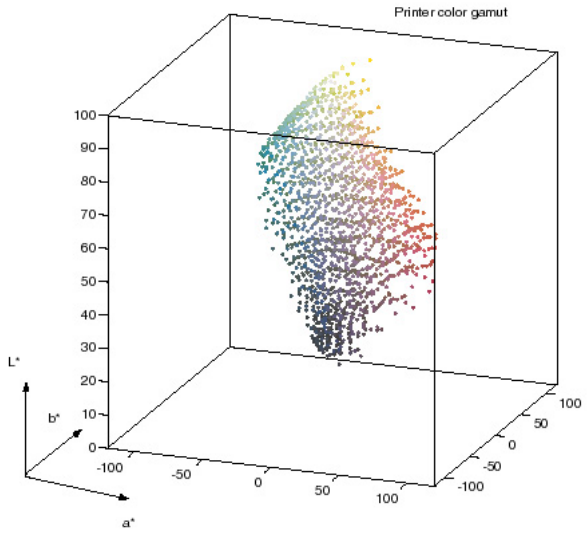

Figure 2 Color gamut of the inkjet printer tested

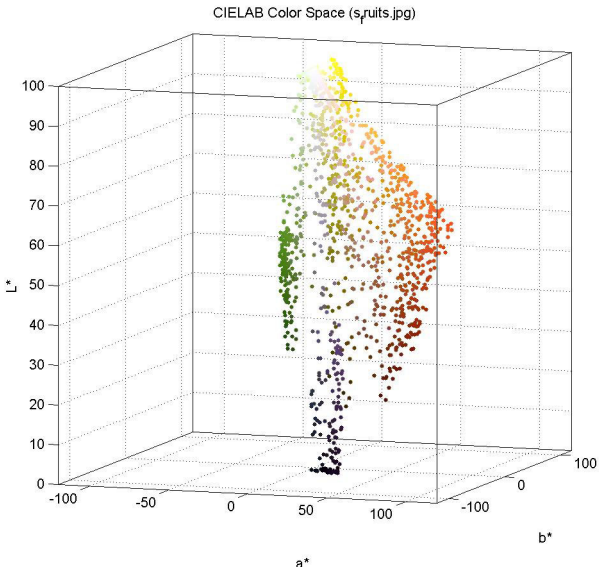

Figure 3 An example of color gamut for one original test image (Fruits)

Finally the tristimulus values transformed into the corresponding CIE L*a*b* coordinates to define inkjet printer gamut (Figure 2).

Image gamut

Two types of test images, including CG and complex, were used in the experiments. The RGB information, initially caught from each input image, was located between 0 and 1 as the monitor's. The corresponding {a*, b*, L*} values, to define image gamut (Figure 3), were then calculated via XYZ tristimulus values which were transformed from sRGB values using a transform matrix (Eqn.1) as follows.

$$\begin{pmatrix} X \\ Y \\ Z \end{pmatrix} = \begin{pmatrix} 100 & 0 & 0 \\ 0 & 100 & 0 \\ 0 & 0 & 100 \end{pmatrix} \begin{pmatrix} 0.4124 & 0.3576 & 0.1805 \\ 0.2126 & 0.7152 & 0.0722 \\ 0.0193 & 0.1192 & 0.9505 \end{pmatrix} \begin{pmatrix} R_{sRGB} \\ G_{sRGB} \\ B_{sRGB} \end{pmatrix}$$

(Eqn.1)

(2) 3D description of gamut shell

A 3D gamut shell was produced by extracting the surface points from the generated color distribution of each of test images, the printer, and the monitor.

Here, the color distribution was segmented into ***m*** lightness planes and ***n*** hue leaves, i.e. ***m**n** L-h segments. The color points having the maximum chroma values at each L-h segments were then extracted to represent the gamut surface points (Chen 2002).

In this research, 24*27 L-h segments were used. The gamut shell, by adding white and black points on the top and bottom, would be then formed by 2***m**n** triangles with ***m**n**+2 surface points (Figure 4).

Afterwards, find each of the surface points and the nearest two neighbors to form a triangle; then each triangle connects to another one; and finally the 3D gamut shell in question is obtained (Figure 5)

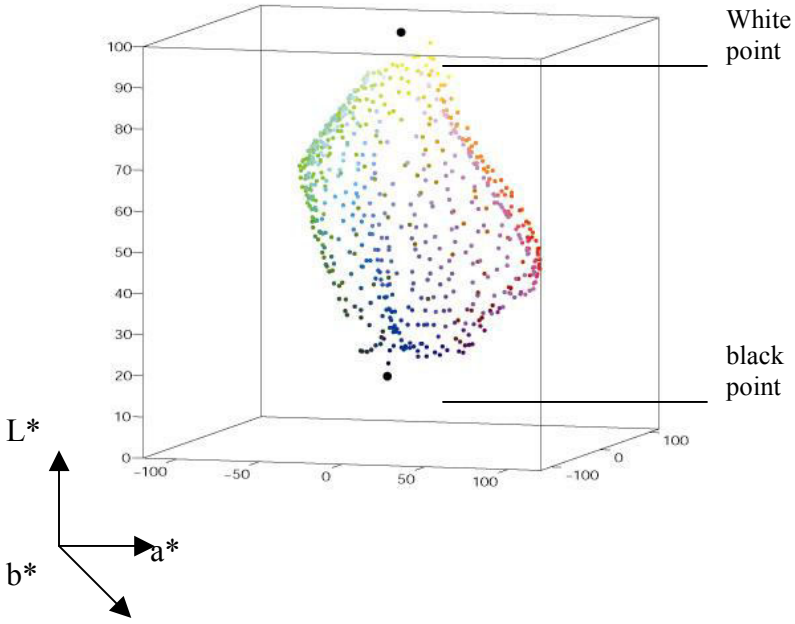

Figure 4 Color gamut surface for the inkjetprinter tested

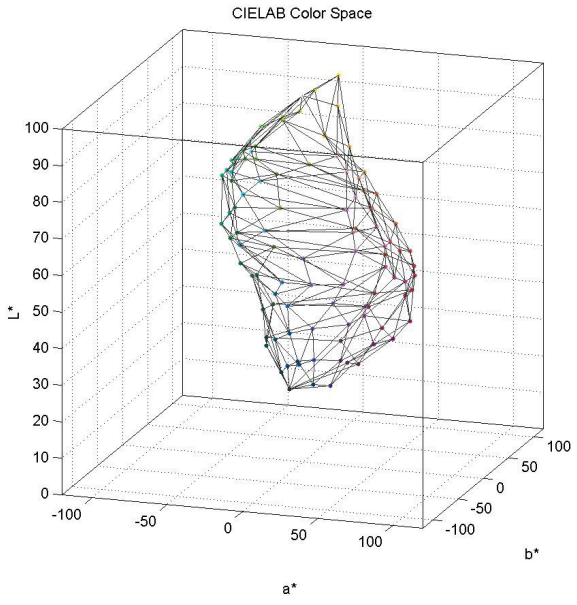

Figure 5 3-D color gamut shell for the inkjet printer tested

(3) Types of mapping

Three kinds of mapping methods were used, including clipping, linear compression, and nonlinear compression (Figure 6)

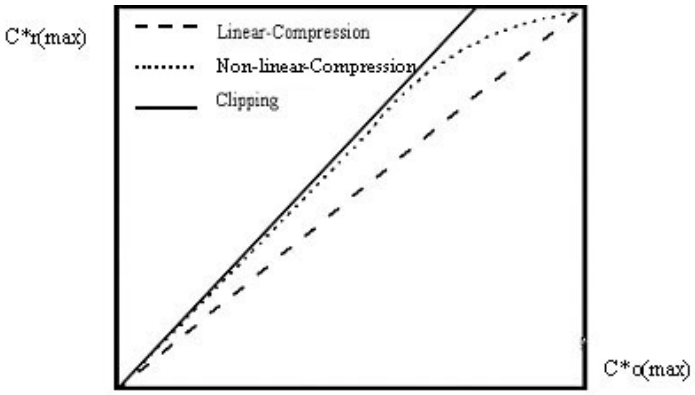

Figure 6 Three kinds of gamut mapping methods

Clipping

All out-of-gamut colors are mapped to the surface of the reproduction gamut, and no changes are made to colors inside the gamut. This method sometimes causes loss of gradation in an image because some of the colors are mapped to the same point, but it maintains most of the image saturation. Clipping is the preferred mapping method if out-of-gamut region is not very important.

Linear-compression

Linearly map all colors of the original gamut into the reproduction gamut. Ideally this method maintains the gradation of test images, but it induces the decrease of images saturation. Therefore lots of image saturations would be decreased if most of color distributions for a test image were near the gamut boundary of the tested reproduction device.

Nonlinear-compression

A non-linear function maps all the colors of the original gamut into the reproduction gamut. This method can minimize the loss of details that occurs with clipping, while retaining the advantage of reproducing accurately most of the common gamut colors.

In this study, the basic Gamma-Compression GMA was directly applied to 3D model in the CIE L*a*b* space (Figure 7 and Eqn.2). As shown in Figure 7, ***i*** denotes a color point on input gamut boundary ; ***o,*** a color point on output gamut boundary ; ***p,*** a focal point ; ***s,*** an input color ; and t, the responding color point needed to obtain. The γ below, $0 \leq \gamma \leq 1$, represents the Gamma-Compression coefficient.

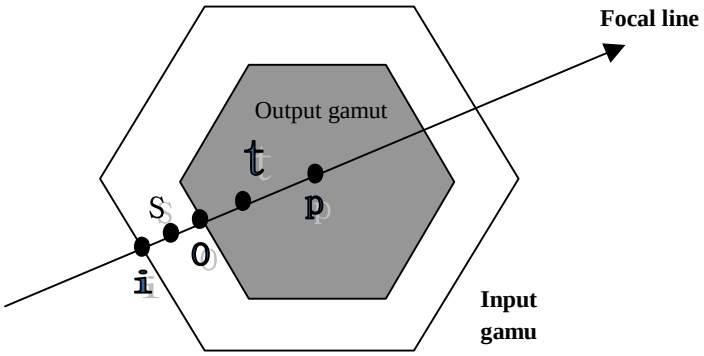

Figure 7 The color gamut section

$$\overrightarrow{pt} = \overrightarrow{po} \cdot \left(\frac{\overrightarrow{ps}}{\overrightarrow{pi}} \right)^{\gamma}$$

Eqn.2

(4) Mapping directions

Generally gamut-mapping directions are dependent on the positions of the focal points. There were two kinds of mapping direction applied here, including single-focal-point and multiple-focal-points.

Single-focal-point

The center of the neutral color (L*=50) was basically chosen as the focal point, and then all the colors of original gamut were mapped toward it. This mapping direction mapped both lightness and chroma simultaneously. It maintained the gradation of the mid-tone but would loss the contrast and gradation at highlight and shadow colors (Figure 8).

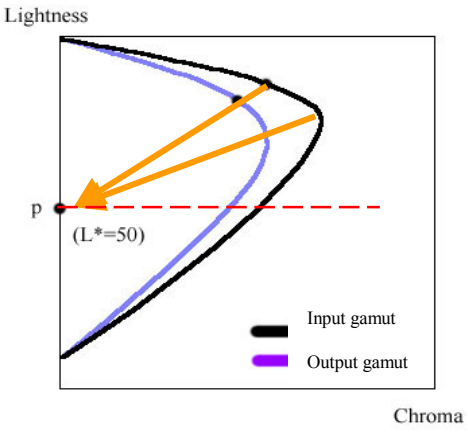

Figure 8 Single-focal-point mapping direction

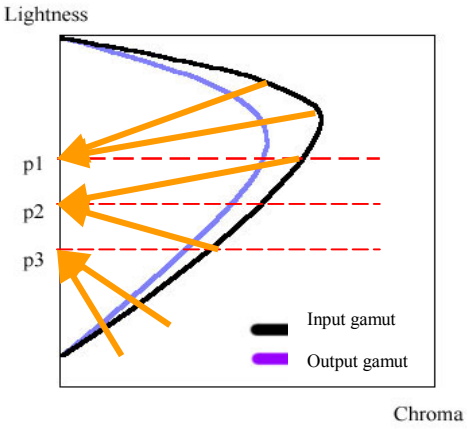

Figure 9 Multiple-focal-points mapping directions

Multiple-focal-points

When applying the approach of multiple-focal-points gamut mapping directions, original gamut was divided into three main parts of highlight, mid-tone and shadow. Gamut compression algorithms were applied on them separately (Figure 9).

This method maintained the saturation for the middle-tone and improved the contrast and saturation imperfection of the highlight and the shadow parts (Lee et al. 2001).

Before applying multiple-focal-points method, the S-type scale method was applied to change the original gamut distributions. The shadow part of original gamut was scaled into the bottom of the reproduction gamut's boundary (Figure 10). The S-type scale method let both gamuts of the original and the reproduction have the same lightness range but still kept the original shadow part's gradation.

(5) Cross points on gamut surface

When an input color mapped towards to a focal point, it would cross with a gamut surface triangle on a cross point.

Finding out the relationship among the triangle's three vertices (v1, v2, v3) and the input point (x4, y4, z4) and the focal point (x0, y0, z0), then the cross point's coordinate (xp, yp, zp) could be computed (Hung 1993).

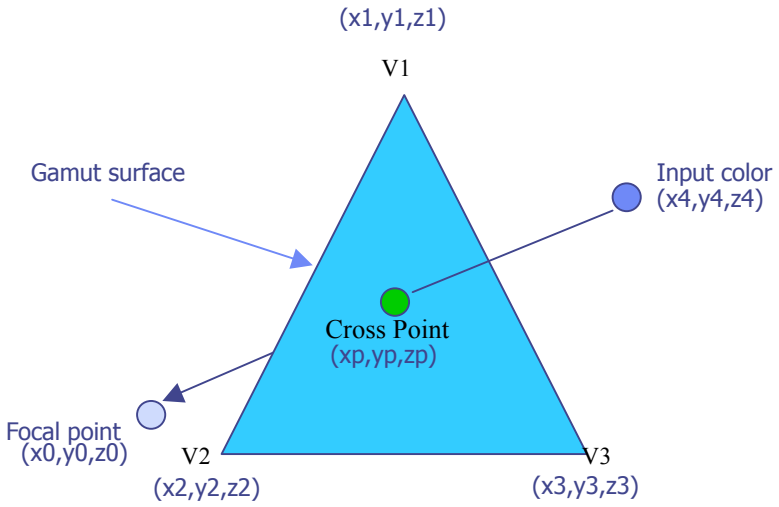

Figure 10 The Cross point on a gamut surface triangle

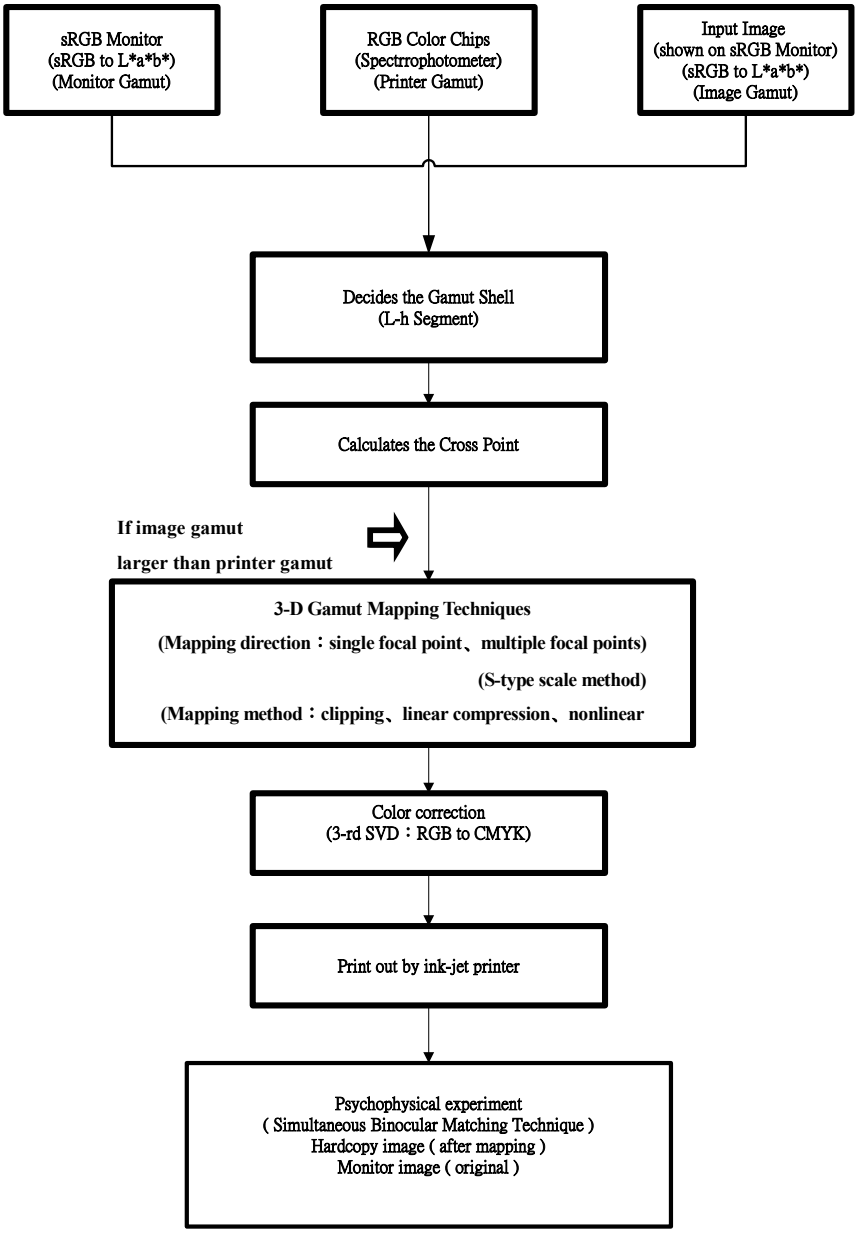

Figure 11 Flow chart for experimental preparation and image processing

Overall, six GMA Algorithms were derived in this study and denoted as follows:

- CS: the Clipping method with a Single focal point.
- LS: the Linear compression method with a Single focal point.
- NLS: the Non-Linear compression method with a Single focal point.
- CM: the Clipping method with Multiple focal points.
- LM: the Linear compression method with Multiple focal points.
- NLM: the Non-Linear compression method with Multiple focal points.

The former 3 models used L*= 50 as the single focal point, whereas the latter 3 ones applied the multiple focal points on three parts of highlight, mid-tone, and shadow separately as mentioned previously.

EXPERIMENTAL PREPARATION

Figure 11 illustrates the process for experimental preparation and image processing. Some details of the computational process and approaches used for GMAs have been described previously.

Device Characterization

As mentioned, a Barco Monitor, which conforms to the sRGB standards (IEC 61966-2-1), was internally set white point to D_{65} and used to display the screen colors or images. A high-end 4-color ink-jet printer (HP 990Cxi) was used to print both of the characterization cube data set (as mentioned earlier) and the reproduced images. A 3-rd SVD (Singular Value Decomposition) method, derived by Lo et al. (1998), was applied to characterize the printer tested to relate between device-dependent RGB data and device-independent L*a*b* values. The measurement equipment was a Gretag spectrophotometer. It measured the spectral reflectance and characterized the device colorants or device colorimetric coordinates for D_{65} illuminant considered.

Image Preparation and Processing

A set of five standard images (ISO/DIS 12640-2) was selected for studying a variety of GMAs models' performance (Figure 12). It consisted of three natural photographed images and two synthetic images (by computer generated). The natural images, identified as "Bride", "Flowers", and "Threads" respectively, include flesh tones, details in the extreme highlights and shadows, neutral colors, brown and wood tone colors which are difficult to reproduce. The synthetic images consist of two computer graphics, named as "Fruits" and "Teapot" respectively.

Figure 12 Five original test images: a) Threads, b) Bride, c) Flowers, d) Fruits, and e) Teapot.

Both computer graphics pictures are three-dimensional and characterized with highlights and/or shadows, large, noise-free, constant hue areas, and gradation areas in which the hue and/or lightness changes very smoothly.

A preliminary evaluation was carried out to have knowledge of both the distribution and the percentage of colors outside the output gamut for each image tested. Table 1 shows the number of test images' colors and the resulted percentage outside the printer gamut for each image.

An image processing software was developed to correlate the sRGB monitor's RGB values (original) to the inkjet hardcopy's RGB values (reproduction) for a

particular GMA model tested on a pixel-by-pixel basis. Each of GMAs was applied only when the image gamut was larger than the printer gamut. As mentioned earlier, the S-scale method, in the testing of multiple mapping directions, re-ranged the input image gamut's lightness into the printer gamut's lightness range.

After gamut mapping, the 3rd SVD algorithm mentioned earlier was applied to calculate the corresponding printer RGB values. The RGB data, transformed into CMYK data via the inkjet printer internal color correction setup, were then used to print out reproduction images.

Table 1 The percentage of colors outside the output gamut for each test image.

Image	Threads	Bride	Fruits	Flowers	Teapot
Image color distribution	8748	11900	9890	7500	9130
Out of printer gamut	4244	1555	4621	4024	5087
Percentage	49%	13%	47%	54%	56%

EXPERIMENT

Viewing Configuration and Condition

The sRGB monitor's white point was set to the chromaticity near the CIE Illuminant D_{65} with a peak luminance of 80 cd/m^2. The printed reproduced images after mapping were viewed in a light booth with the same color temperature and peak luminance as sRGB monitor's setting, under a dim viewing surround where the level of ambient illumination is approximately near 64 lux.

Viewing Technique

A psychophysical experiment had been carried out to make comparisons of color appearance matching between the original images shown on sRGB monitor and the printed reproduced images after mapping. A forced-choice paired comparison method, with simultaneously binocular viewing technique, was employed in this experiment. It was based on the judgments made for the color-fidelity quality of test images reproduced by GMAs of interest. A panel of 10 observers viewed a paired of reproduced hardcopies, and judged which of the two gave a better match (i.e. color fidelity) to the original softcopy. In addition, they also accessed the degree of match of the softcopy against the hardcopy using a predetermined equi-interval of 7-point category scale for overall color fidelity (Table 2). The order of the pairs was randomized when presented to each

observer. The 7-point category scale for color fidelity is defined from 1 (exact match), through 4 (acceptable match) to 7 (awful match) as below.

Table 2 A predetermined equi-interval of 7-point category scale

Category Rank	1	2	3	4	5	6	7
Word Category Scale	Exact Match	Good Match	Moderate Match	Acceptable Match	Poor Match	Bad Match	Awful Match

DATA ANALYSIS

The resulted visual data were analyzed using the laws of comparative judgment (Thurstone 1927, Bartleson and Grum 1984). Therefore a series of interval scales (mean *Z* score values) were generated to define both the ranking order of the algorithms performance and a gauge of the relative difference between the techniques.

A higher value indicates that better matching is obtained between the original image shown on the sRGB monitor and the reproduced image after mapping by the inkjet printer. Complementarily mean scale values of category for each of GMA models tested would be averaged from the visual raw data accessed from all 5 images using the categorical method. Those were used to identify models' categorical ranking in color fidelity.

RESULTS AND DISCUSSION

The results in terms of both z-score and category scales obtained using the law of comparative judgment are summarized in Table 3. The overall results are also depicted in Figure 13. The ordinate shows the interval psychophysical scale (*z* score) calculated statistically from the experimental data. The abscissa represents the z score of models of interest, and each line drawn (error bar) indicates the 95% confidence limit (CL) of the corresponding model (Lo et al. 1996). A model evaluated is considered not to be significantly different from another if its mean z score is within the 95% confidence limit (CL, i.e. ±2 units of standard deviations) of the other. Hence, these would be ranked in the same order.

Table 3 Paired comparison results in terms of both z-score and category scales based on the judgments made for the overall color-fidelity accuracy obtained from all the 5 test images combined. (95% CL = ±0.3099 for each image, 95% CL = ±0.1385 for overall images)

Image	Z-score scales					
	CS	LS	NLS	CM	LM	NLM
Threads	**-0.18**	**-0.65**	**-1.49**	**0.54**	**0.42**	**<u>1.37</u>**
Rank	4	5	6	2	2	1
Bride	**-0.59**	**0.30**	**-1.31**	**-0.59**	**0.89**	**<u>1.31</u>**
Rank	4	3	6	4	1	1
Fruits	**-0.78**	**1.00**	**-1.28**	**-0.29**	**0.07**	**<u>1.28</u>**
Rank	5	1	6	3	3	1
Flowers	**-1.17**	**-0.88**	**-0.06**	**-0.18**	**0.82**	**<u>1.47</u>**
Rank	5	5	3	3	2	1
Teapot	**-1.11**	**-1.00**	**-0.39**	**0.39**	**0.72**	**<u>1.39</u>**
Rank	5	5	3	2	2	1
Overall Z-score	**-0.90**	**-0.35**	**-1.03**	**-0.01**	**0.70**	**<u>1.59</u>**
Rank	5	4	5	3	2	1
Average category scale	5	4	5	4	3	2

Note: The underlined figure indicates the best performing model for a particular image or overall 5 images, and CL represents confidence limit.

The results, obtained from both every image and overall images, showed that the NLM model (Non-linear compression gamut mapping algorithm with multiple focal points) had the highest interval scales among six models tested. This algorithm minimized the loss of details that occurred with clipping, while retaining the advantage of reproducing accurately most of the common gamut colors. Moreover three models, which applied the multiple-focal-points approach, including CM, LM, and NLM, all performed better than acceptable match.

In addition, the chosen positions of the multiple focal points, which depends on the color distribution of the original image used, would concurrently affect the GMAs' performance. Non-linear compression with well chosen multiple mapping directions directly in 3-D color space could yield good appearance match of reproductions to their corresponding originals.

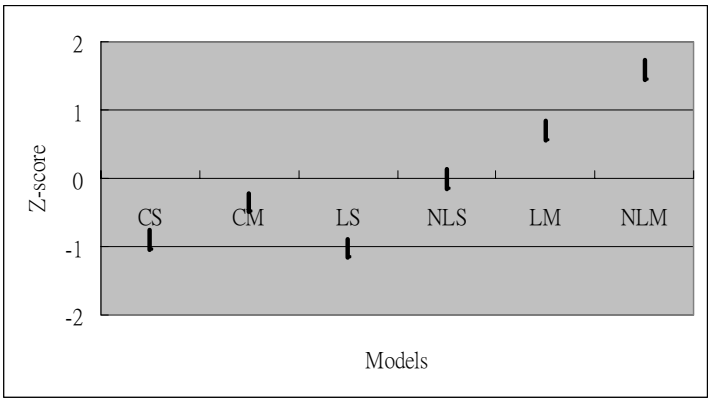

Figure 13 GMA models' performance evaluated using the law of comparative judgment for the overall color-fidelity accuracy of all the 6 test images (including 95% confidence limit)

CONCLUSIONS

A 3-D Gamma-Compression GMA, based on image-dependency, was proposed. It was shown that the GMA coupled with both of non-linear 3-D gamut compression and multiple-mapping-directions approaches outperformed other five models tested. It was especially evident to complex images but less evident to CG images especially that are with fewer gradations.

It is a key point that a true 3-D GMA gives seamless mapping without color segmentation, thus without causing unnatural artifacts as compared with 2-D GMAs in L*-C* planes in terms of hue division, or 3-D GMAs based on device-dependency.

Comparing the 3-D mapping effects in terms of single versus multiple mapping directions, It was found that the GMA applied multiple mapping directions, which is dependent on image's color distribution, could enhance the perception on both lightness and chroma of test images after mapping. It is superior to the GMA mapped toward a single mapping direction.

Non-linear Gamma-Compression could minimize the loss of detail that occurred with clipping, while retaining the advantage of reproducing accurately most of the common gamut colors.

The further work is to design a program to automatically decide the multiple focal-point positions according to the original images dependency. Moreover the image manipulation for gamut mapping will be performed in the perceptually

significant correlate dimensions of an existing advanced color appearance model instead of the CIELAB color space.

REFERENCES

1. Bartleson, C. J. and Grum, F, Visual Measurement, Academic Press, Inc, *Optical Radiation Measurement Volume 5, pp. 455-467 (1984).*
2. Chen, H. S., Three-dimensional Gamut Mapping Method Based on the Concept of Image Dependence, *Journal of Imaging Science and Technology, Volume 46, Number 1, January/February, pp. 44-62 (2002).*
3. Hung, P. C., Colorimetric Calibration in Electronic Imaging Devices Using a Look-Up-Table Model and Interpolations, *Journal of Electronic Imaging 2(1), pp. 53-61 (January 1993).*
4. IEC 61966-2-1: 1999, Color Measurement and Management in Multimedia Systems and Equipment – Part 2-1: Default RGB Colour Space – sRGB, *IEC (1999).*
5. ISO/DIS 12640-2, Graphic Technology – Prepress Digital Data Exchange – XYZ/sRGB Standard Colour Image Data (XYZ/SCID), *ISO (2000).*
6. Katoh, N. and Ito, M., Applying Non-linear Compression to the Three-dimensional Gamut Mapping, *The Seventh Color Imaging Conference：Color Science, Systems, and Applications, pp. 155-158 (1999).*
7. Lee, C. S., Park, Y. W., Cho, S. J., and Ha, Y. H., Gamut Mapping Algorithm Using Lightness Mapping and Multiple Anchor Points for Linear Tone and Maximum Chroma Reproduction, *Journal of Imaging Science and Technology, Volume 45, Number 3, May/June, pp. 209-223 (2001).*
8. Lo, M. C., Chiang, R., The Characterization Models for Multi-colored CMYKRGB, *TAGA Proceeding, pp. 242-254 (1998).*
9. Lo, M. C., Luo, M. R., Evaluating Color Models' Performance Between Monitor and Print Images, *Color research and Application, Volume21, Number 4, August pp. 227-291 (1996).*
10. Thurstone, L. L., A Law of Comparative Judgement, *Psychological Review*," ***34**, pp. 273-286 (1927).*